DSC Assessment on Curing Degree of Micron-scaled Adhesive Layer in Lamination-pressed Flexible Printed Circuit Panels

Kok-Tee Lau, Hoi Ern Kok*
Fakulti Teknologi Kejuruteraan Mekanikal dan Pembuatan,
Universiti Teknikal Malaysia Melaka,
76100 Durian Tunggal, Melaka, Malaysia
**ktlau@utem.edu.my*

Nur Hazirah Rosli
MFS Technology (Malaysia) Sdn. Bhd., 75350 Batu Berendam,
Melaka, Malaysia.

ABSTRACT

Continuous monitoring and optimisation of the lamination process are critical in negating flexible printed circuit (FPC) delamination risk during operation. The main QC inspection criterion of the lamination adhesive's curing degree is adhesive thickness. However, this method is prone to measurement error due to poor microscopy image definition and the inspector's measurement parallax error. The feasibility of using thermal characterisation to measure the difference in curing degrees of micron-scaled adhesive layer of laminated FPC was investigated. Differential scanning calorimetry (DSC) and thermogravimetric analysis (TGA) were used according to IPC standards. Polyimide-epoxy adhesive coverlays were laminated onto both sides of FPC at 120 kgf/cm^2 pressure and 180 °C temperature for 120 s. Then, the coverlays were subjected to oven curing at 150 °C for 60 min. The DSC detected a small difference in the curing degree of adhesive layers in the two cured FPC laminated in different laminating-press openings (T1 and T2). T2 had a glass transition temperature (T_g) of 106.5 °C, which was higher than that for T1 (105 °C), thereby suggesting that the former had a higher curing degree than the latter. This result was consistent with the adhesive thickness measurement result of the DSC samples. The adhesive thickness of T2 was smaller (30.97 µm) than that of the T1 (31.76 µm). T2 had a higher curing degree than T1 because of the larger shrinkage percentage. In comparison with DSC, TGA

ISSN 1823-5514, eISSN 2550-164X
© 2021 College of Engineering,
Universiti Teknologi MARA (UiTM), Malaysia.
Received for review: 2021-02-03
Accepted for publication: 2021-08-19
Published: 2021-09-15

was unable to detect the curing degree difference between the samples because of the undetected weight loss resulting from the adhesive curing.

Keywords: *Flexible printed circuit; Epoxy adhesive; Coverlay lamination; Thermal properties; Curing degree*

Introduction

The increasing number of applications of flexible and stretchable electronics has led to high demand for flexible printed circuit boards (FPC) [1]–[5]. FPC is developed using copper-clad laminate (CCL) to create electronics circuit patterns and simultaneously provide mechanical strength to withstand deformation during operation [6]. The quality control process improvement on FPC largely focuses on the use of vision-based inspection technologies to detect defects in the FPC circuit [7]–[9]. Lamination is performed at the last stage of FPC manufacturing to increase the mechanical robustness of FPC [6]. Previous risk assessment findings on the escape defects from unknown FPC suppliers of a flexible printed circuit board (FPCB) for smartphones showed a defective rate between 1.50% and 4.99%, but failure modes can be detected by operators' self-check [10]. The two main failure modes for flexible electronic devices are crack propagation and delamination, which are generally more common in the conductive layer than in the polyimide structure [11].

Escape defects contributed by the FPC supplier should be reduced to as few as possible through continuous monitoring and optimisation of the FPC manufacturing process [10]. Thus, lamination integrity is critical in protecting the FPC circuit; it negates FPC failure mode risk during subsequent FPCB assembly at the OEM stage. During lamination, heat and pressure are applied simultaneously in a controlled manner to bond a protective coverlay onto the surface of the FPC's circuit pattern [6]. A typical coverlay is a two-layer material composed of a polyimide sheet as base material and a suitable thermosetting adhesive [6]. The commonly used adhesives are epoxy- and acrylic-based; they require different lamination temperatures and pressure parameter settings [6]. Optimised parameters ensure good conformation (no air entrapment) of the adhesive layer on the circuit pattern and sufficient curing degree or degree of cure of the adhesive after lamination [12].

Curing degree increases with increasing adhesive viscosity [13]. Careful setting of lamination temperature and pressure enables the smooth flow of the adhesive onto the circuit pattern, thereby eliminating void formation risk. Currently, adhesive thickness is measured according to the IPC standard and is the main QC inspection criterion of the lamination adhesive's curing degree [6, 14]. When a coverlay adhesive is applied to the FPC under high pressure and temperature, the thickness of the adhesive layer reduces dimensionally as a result of increased curing degree. Despite the feasibility of

adhesive thickness measurement by microscopy technique, the method is prone to measurement error caused by thickness tolerance error of the as-received coverlay-adhesive, limitation in microscopy image definition or inspector's measurement parallax error [15].

Several alternative methods have been used to measure adhesive curing degree, as follows: change in adhesive strength is determined by peel strength tester; viscoelasticity is determined by rheometer; the functional group is determined by FT-IR, and heating value is determined by thermal analysis instruments [16]. Although adhesive strength can be determined directly using a peel strength tester, the sample preparation is tedious because of the micron-scale thickness of the two adhered layers [17]. Rheometer characterisation for adhesive viscoelasticity is not *in-situ*, and the sample at a sufficient amount needs to be extracted for testing [18]. Similarly, sample preparation for FT-IR spectrophotometer is tedious, because the challenge of signal contamination from the FPC's polyimide layer needs to be addressed [19].

Compared with these techniques, DSC and TGA require only a small sample; the sample is cut from the inspected large-area FPC without additional sample preparation steps (*in-situ*) [20]. Furthermore, technological advancement in the DSC and TGA equipment in terms of their measurement capabilities creates a new opportunity for faster and more accurate detection [21]. DSC and TGA data analyses require basic knowledge of thermodynamics and materials' quantitative data [22]. Thus, the use of DSC and TGA in the quality control of manufactured products has become popular. The use of DSC and TGA in studies on the manufactured FPC coverlay adhesive's curing degree has not been reported.

DSC and TGA can be used as qualitative characterisation techniques for root-cause analysis to verify if the delamination or air entrapment failures of the defect FPC could be traced to the inadequate adhesive curing. Inadequate curing degree of the adhesive of the laminated FPC is a major contributor to the high delamination failure risk in lamination samples [12]. An adhesive's curing degree correlates directly with its polymerisation or molecular cross-linking density and thus could be picked up easily as a jump in the DSC baseline (e.g., at glass-transition temperature) [22].

Conventional thickness measurement has been used as a cost-effective technique in the manufacturing industry to qualify the laminated FPC product. Nevertheless, the technique has a limitation to detect small curing degree variation, particularly on thin and micron-scaled adhesive layers. The current paper investigates the feasibility of using DSC and TGA as qualitative characterisation tools to assess the curing degree of lamination pressed FPC. Furthermore, this investigation intends to validate the inadequate adhesive curing using DSC or TGA for the case where the laminating pressed FPCs produced by different laminating press openings displays insignificant shrinkage's variation in the cured adhesive layers.

Methodology

Laminating press and cure processes

Coverlay-adhesive sheet (i.e., polyimide (PI) sheet thickness = 12.7 µm, epoxy adhesive thickness = 35.56 µm and model = ThinFlex-Q2, Q-0514TA-mb, TopFlex Co.), which had 5-mm diameter holes at its four corners and centre, were used for the lamination of FPC. The CAS number of the halogen-free epoxy adhesive material was not disclosed by the supplier due to confidentiality issues [23]. Before conducting the laminating press, the coverlay-adhesive sheet and FPC were stacked in sequence with other elements (from top-to-bottom) as follows: steel plate, kraft paper, HTRF releasing paper, coverlay sheet, blank doubled-sized FPC, coverlay sheet, HTRF releasing paper, kraft paper and steel plate. A similar stack arrangement was prepared carefully to ensure consistency in the lamination quality.

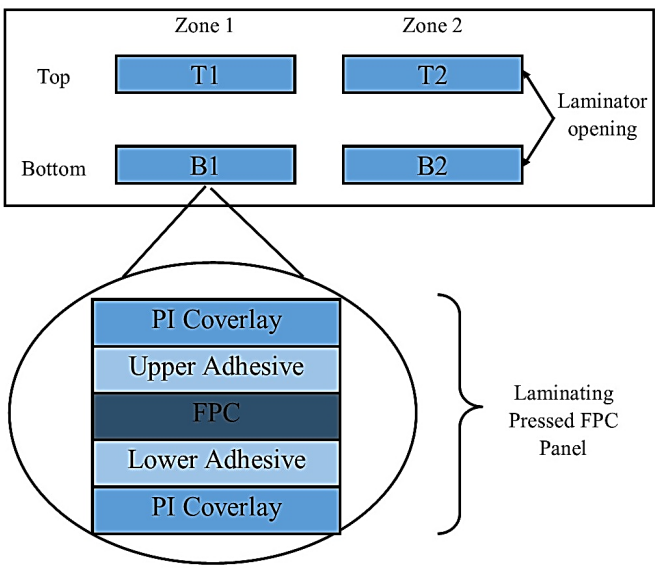

Figure 1: Lamination-pressed FPC obtained from different laminating press openings were labelled accordingly as T1, T2, B1 and B2. The zoom-in view shows a schematic cross-sectional view of one of the laminated FPC.

The lamination press of the stacks was performed by using the four-opening laminating press (platen size = 545 × 660 mm, Beyond China) under fast and hot-pressing conditions, as recommended by the coverlay supplier [24]. All four openings (see Figure 1) were set at a temperature of 180 °C and

pressure of 120 kgf/cm^2 for a time interval of 120 s. Then, all stacks underwent post-cure condition using an oven (model Gol-8D) at 150 °C for 60 min. After cooling, the cured laminated FPC sheets were labelled based on their laminating press's opening location, as shown in Figure 1. For example, the sample obtained from the top opening at zone 1 was labelled as T1.

Characterisation methods

Adhesive thickness was characterised according to IPC TM-650, 2.2.18.1 standard [25] to quantify the curing degree of adhesive in the laminated FPC. IPC stands for the Institute for Interconnecting and Packaging Electronic Circuits, which develops standards for the assembly and production requirements of electronic equipment. Five 1 cm^2 strips were cut from each of the T1, T2, B1 and B2 FPCs at different planar regions (see Figure 2). The strips were then subjected to a conventional cross-sectioned sample preparation process, which involved cold resin mounting followed by cross-sectioning and surface polishing of the FPC sample. The images of a polished and smooth cross-section of the samples were captured using a 3D laser scanning microscope (VK-X200 series, Keyence). Each of the upper and lower adhesive layers displayed in the cross-sectioned samples was measured using VK-Analyser software. After that, the average and standard deviation of the measured data from the five planar regions of the upper and lower adhesive layer of T1, T2, B1 and B2 samples were calculated.

To assess the validity of the thickness measurement data in relation to curing degree variation, the adhesive layer of laminated T1 and T2 FPC were characterised by TGA 1 from Mettler Toledo and DSC is characterised using Jade DSC from PerkinElmer. T1 and T2 FPCs were chosen to investigate the curing degree, because the former and the latter had the smallest and the largest thickness variations, respectively. TGA and DSC characterisations were performed according to IPC TM-650, Method 2.3.40 [26] and IPC TM-650, Method 2.4.25 [27]. Both characterisations were conducted in an inert nitrogen gas environment. Samples for characterisations were cut from the centre region of their respective laminated T1 and T2 (Figure 2). The respective initial weights were 7.27 and 6.41 mg for TGA and 10.4 and 9.9 mg for DSC. DSC characterisations were performed by heating the DSC sample from room temperature to 400 °C and then cooling it to ambient temperature. In contrast, TGA characterisation was only performed during heating until 800 °C.

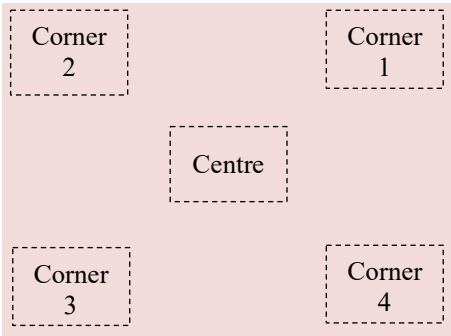

Figure 2: Bird's eye view shows that thickness measurement samples were cut from the five planar regions (indicated by the dashed boxes) on a single laminated FPC. Only the Centre region was used for DSC and TGA characterisations.

Result and Discussion

Thickness and shrinkage percentage's averages of the upper and lower adhesive layers (Figure 1) obtained from the five planar regions (Figure 2) of the cured T1, T2, B1 and B2 samples were plotted in Figure 3. The shrinkage percentage of each measured adhesive layer was calculated using Equation 1 adapted from the volume shrinkage equation [28].

$$\text{Shrinkage } \% = \left(1 - \frac{\text{cured adhesive thickness}}{\text{uncured adhesive thickness}}\right) \times 100\% \quad (1)$$

where thickness is in µm, and 35.56 µm is the uncured adhesive thickness (as provided by the manufacturer). The shrinkage percentage's error bar represents the degree of adhesive thickness's variation along with the planar FPC sheet, thus provided an analogy of volume shrinkage of the cured adhesive thickness.

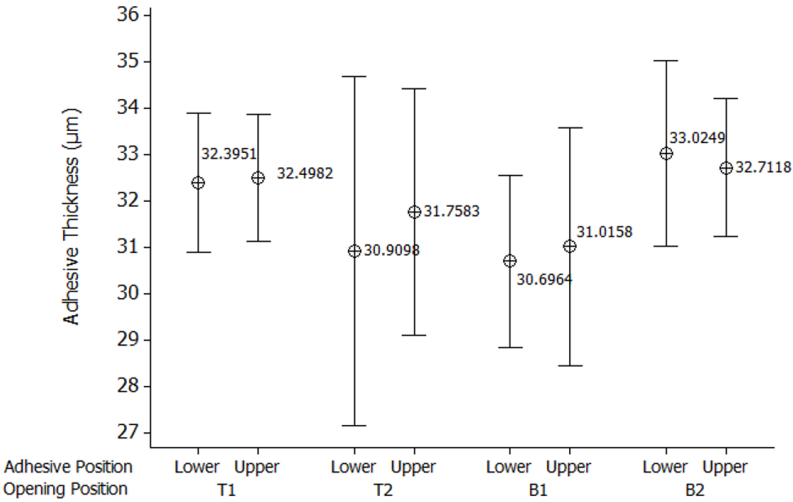

(a)

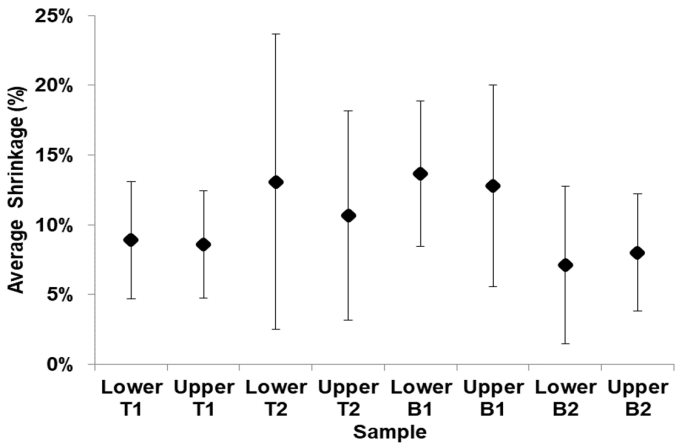

(b)

Figure 3: Interval plot with a 95% confidence interval of the: (a) lower and upper adhesives' thicknesses, and (b) shrinkage percentage of different lamination pressed FPC samples. Data point represents the average value, and error bar indicates the standard deviation.

The average adhesive thicknesses of the four laminated FPC samples shrunk between 7% and 14% from the original thickness of 35.56 µm after curing. The adhesive underwent shrinkage because of the epoxy polymer cross-linking process. One-way ANOVA analysis (see Table 1) shows that the

P-value is 0.32 and more than 0.05 at a 95% confidence level. This result implied the lack of significant difference between the average lamination-pressed (cured) adhesive thickness with respect to the laminating press opening positions and adhesive layer positions (upper and lower adhesive layers) [29, 30]. Nevertheless, T2 samples' thickness for the Lower adhesive layer had the largest margin of error, which varied from 27.1 µm to 34.6 µm. The T1 sample's thickness (for the Upper adhesive layer) had the lowest variation, which varied from 31.1 µm to 33.9 µm. Cross-sectional images of Figures 4(a) and 4(b) show the adhesive layer thickness of T2, which varied from 28.0–30.7 µm at Corner 2 to 35.6 µm at Corner 4. Images obtained at Corner 2 and Corner 4 regions respectively exhibited the smallest (thinnest) and largest (thickest) adhesive layers after laminating press. The variation of measured adhesive thickness throughout the different locations in the T2 sample, including data from the Corner 2 and 4 regions were represented as the interval plot's error bar of Figure 3(a) which was determined statistically at a 95% confidence level.

Table 1: One-way ANOVA analysis at 95% confidence interval for the adhesive thickness data of Figure 3(a)

Source of Variation	SS	df	MS	F	P-value	F_{crit}
Between Groups	28.77	7	4.11	1.22	0.32	2.31
Within Groups	108.18	32	3.38			
Total	136.95	39				

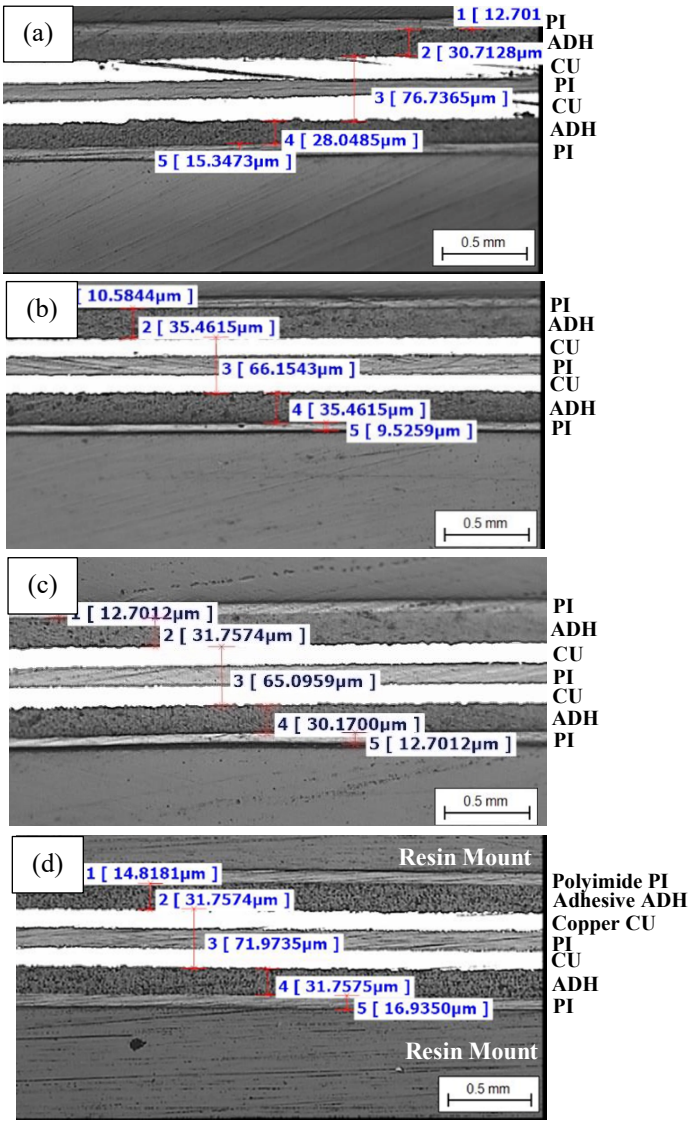

Figure 4: Cross-sectional image of T2's adhesive layers cut from (a) Corner 2 (thinnest adhesive) and (b) Corner 4 (thickest adhesive) regions. Cross-sectional images of T2 and T1 samples' centre region before DSC and TGA characterisations are shown in (c) and (d).

According to the adhesive thickness measurement method, the large variation in cured adhesive thickness of T2 samples suggested that the adhesive's curing degree varied more significantly over the FPC area for T2 compared with the other three samples. However, ANOVA analysis showed that the average adhesive thickness of samples produced by the four openings had no significant difference. This analysis result suggested that the thickness variation was random and was not caused by systematic error sources, such as sheet's position accuracy, non-uniform applied temperature and pressure distribution throughout the lamination press platen [6]. As mentioned in the previous section, the possible sources of the random error were the thickness variation of the as-received raw materials, e.g. coverlay-adhesive has a thickness tolerance of ±10% [24], microscopy image definition limitation or the inspector's measurement parallax error [15].

It is important to validate the inadequate adhesive curing using DSC or TGA when the laminating-pressed FPC produced by different laminating press openings displays insignificant variation in shrinkage percentages (as shown by Figure 3(b)) after adhesive layer curing. When the curing process was performed by lamination press followed by curing at 150 °C, the combined effects of pressure, as received cover lay thickness tolerance and temperature resulted in a small curing degree variation in the adhesive layer. Thus, assessing the validity of thickness measurement data by DSC and TGA characterisations is important. For the sake of this investigation, T1 and T2 samples were chosen for comparison because their SEM micrographs showed an obvious discrepancy in the thickness variation. SEM micrographs of the T1 show adhesive layer thicknesses of 31.76 µm, which was slightly thicker than T2 with a value of 30.97 µm, as shown in Figures 4(c) and 4(d).

The DSC and TGA assessments were performed on small cut from the centre region of the T1 and T2 sample. DSC curves of T1 and T2 samples were compared only between 75 °C and 120 °C (Figure 5) to clearly reveal the weak glass transition temperature (T_g) peaks. T_g of T1 were observed as a slight jump in the DSC baseline at ~88.5 °C during heating and 105 °C during cooling. However, the T_g of T2 only appeared on the cooling curve at 106.5 °C. The obtained T_g values were near the previously reported T_g values [16, 30]. T_g has been widely used as a measure of the degree of crosslink in epoxy adhesives [22]. Higher T_g on the cooling curve for T1 indicated an increase in crosslink density of T1's adhesive after the heating process. Menczel et al. [22] argued that T_g depends on the polymer chains' mobility; polymers possessing more mobile chains have a lower T_g value. A comparison between T1 and T2 samples during cooling however showed that the latter has a higher T_g (1.5 °C difference), thereby showing a higher curing degree. The DSC results agreed with the adhesive thickness data of the T1 and T2 samples, as shown in Figures 4(c) and 4(d). The consistency of DSC's T_g value with the thickness data proved the effectiveness of using the DSC technique to differentiate the cure

quality of cured laminated FPC sample of Figure 3, which demonstrated a thickness difference of 0.79 µm between the two DSC samples.

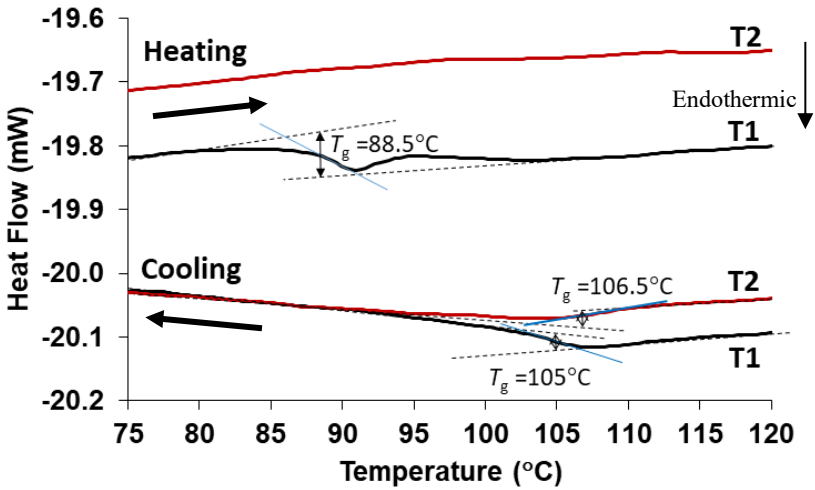

Figure 5: Glass transition temperature (T_g) of epoxy in T1 and T2 samples during the heating and cooling stages of DSC curves. Bold arrow shows the direction of temperature change during DSC measurement.

TGA results (Figure 6) only exhibited observed weight loss at temperatures above 350 °C. T2 recorded a lower weight loss (~11.9%) and a higher pyrolysis temperature (383.05 °C) than T1. A slight weight loss at 260 °C was observed in the T1 and T2 samples probably due to the epoxy adhesive's decomposition [31]. The larger weight loss of above 350 °C may be due to the polyimide's decomposition because it had a larger initial weight percentage than the epoxy adhesive. The claims on epoxy and polyimide decompositions were supported by Wypych data, which showed that their maximum service temperatures were 350 °C and 500 °C, respectively [31]. According to the current study's TGA finding, TGA was unable to detect the curing degree difference among the varied samples because of the extremely low weight loss caused by adhesive pyrolysis.

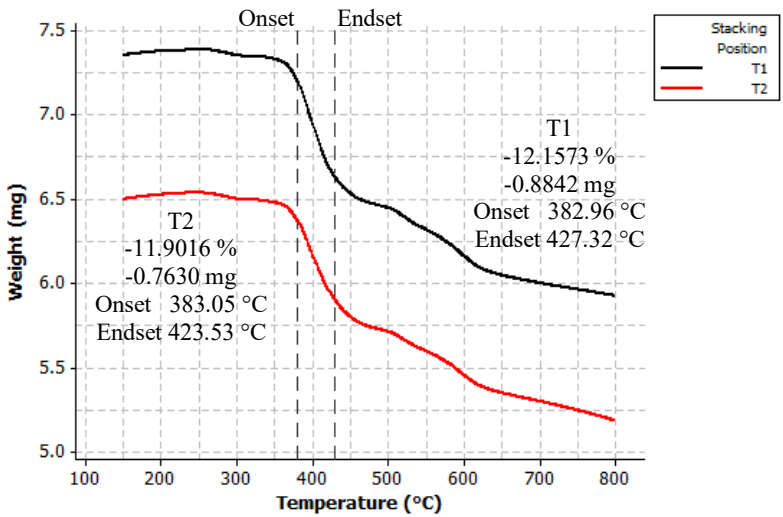

Figure 6: TGA curve.

Conclusion and Recommendation

DSC can detect the differences in the curing degree of the micron-scaled adhesion layer of two cured FPCs laminated at different laminating-press openings (T1 and T2). This result was consistent with the adhesive layer thickness measurement results obtained from the same laminated samples. The adhesive layer of the T1 sample (31.76 µm) was thicker than the sample from T2 (30.97 µm). TGA was unable to characterise the curing degree of epoxy adhesive in the cured and laminated FPC sample because of the extremely low weight loss caused by adhesive pyrolysis. Future work needs to investigate the effects of stacking conditions (stacking materials and sequence) on the curing degree of the laminated FPC adhesive layer using DSC. The outcome of the paper can be used to minimise the adhesive layer non-uniformity under improper stacking conditions.

Acknowledgement

The authors wish to thank MFS Technology for providing sample preparation and 3D laser microscopy characterisation facilities. They would like to acknowledge Universiti Teknikal Malaysia Melaka for the technical support in DSC and TGA characterisations.

References

[1] Z. Cui, "Printing practice for the fabrication of flexible and stretchable electronics," *Science China Technological Sciences*, vol. 62, no. 2, pp. 224-232, 2019.

[2] R. Dahiya, "E-Skin: From Humanoids to Humans," *Proceedings of the IEEE*, vol. 107, no. 2, pp. 247-252, 2019.

[3] Chung, K. -C. and B. W. Moon, U.S. Patent No. 10 887 997, 5 January 2021.

[4] M. M. Mahat, M. F. Aizamddin, N. C. Roslan, M. A. Kamarudin, S. N. I. Omar, M. I. A. Halim and M. M. Mazo, "Conductivity, morphology and thermal studies of polyaniline fabrics," *Journal of Mechanical Engineering*, vol. 9, no. 1, pp. 137-150, 2020.

[5] M. F. M. Sharif, A. A. Saad, F. C. An, M. Y. T. Ali and Z. Samsudin, "Effect of Stretchable Circuit Deformation on Its Electrical Performance for Automotive Lighting Application," *Journal of Mechanical Engineering*, vol. 4, no. 2, pp. 279-287, 2017.

[6] J. Fjelstad, Flexible Circuit Technology, 4th ed., Seaside: BR Publishing, 2011.

[7] W. Luo, J. Luo and Z. Yang, "FPC surface defect detection based on improved Faster R-CNN with decoupled RPN," *2020 Chinese Automation Congress (CAC)*, IEEE, Shanghai, 2020, pp. 7035-7039.

[8] X. Tao, D. Zhang, W. Ma, X. Liu and D. Xu, "Automatic metallic surface defect detection and recognition with convolutional neural networks," *Applied Sciences*, vol. 8, no. 9, pp. 1575, 2018.

[9] Z. Zhao, B. Li, F. Gao, L. Chen and M. Xin, "Online vision system for battery FPC connector defect detection based on active shape model template matching," *Proceedings of SPIE: Tenth International Symposium on Precision Engineering Measurements and Instrumentation*, vol. 11053, pp. 11053 0Z, 2019.

[10] S. Krasaephol and P. Chutima, "Quality control process improvement of flexible printed circuit board by FMEA," *IOP Conference Series: Materials Science and Engineering*, vol. 311, no. 1, pp. 012009, 2018.

[11] B. P. DeFigueiredo, T. K. Zimmerman, B. D. Russell and L. L. Howell, "Regional stiffness reduction using lamina emergent torsional joints for flexible printed circuit board design," *J. Electronic Packaging*, vol. 140, no. 4, pp. 041001, 2018.

[12] J. J. Licari and D. W. Swanson, Adhesives technology for electronic applications: materials, processing, reliability, 2nd ed., Norwich: William Andrew, pp. 194-233, 2011.

[13] T. Löbel, D. Holzhüter, M. Sinapius and C. Hühne, "A hybrid bondline concept for bonded composite joints," *International Journal of Adhesion and Adhesives*, vol. 68, pp. 229-238, 2016.

[14] K. -T. Lau, H. E. Kok, H. E. B. A. Maulod, N. Z. B. A. Latiff, A. N. B. A. Aziz and N. H. B. Rosli, "Effect of Laminating Press's Opening-Stacking Position on Adhesive Thickness in Coverlay/Adhesive/Flexible-Printed-Circuit Sheet," *Journal of Engineering Technology and Applied Physics*, vol. 1, no. 1, pp. 1-3, 2019.

[15] M. E. Keeble, "Error and Uncertainty in Metallographic Measurement," in 100 Years of E04 Development of Metallography Standards, West Conshohocken: ASTM International, 2019, pp. 53-65.

[16] S. Tanaka, T. Kiryu and H. Takebe, "Curing Degree Evaluation of Reactive Adhesives Using Measurement Devices," *ThreeBond Technical News*, vol. 1 July 2015, pp. 1-8, 2015.

[17] M. Valori, V. Basile, S. P. Negri, P. Scalmati, C. Renghini and I. Fassi, "Towards the Automated Coverlay Assembly in FPCB Manufacturing: Concept and Preliminary Tests," *in Smart Technologies for Precision Assembly: 9th IFIP WG 5.5 International Precision Assembly Seminar*, IPAS 2020, Cham: Springer Nature, pp. 36-50, 2021.

[18] M. Jährling, "The curing behaviour of reaction resin compounds," Application Note LR-12, [Online]. Available: ThermoFisher Scientific, https://www.thermofisher.com. [Accessed Apr 26, 2021].

[19] PerkinElmer Life and Analytical Sciences," Applications and Design of a Micro-ATR Objective," Technical Note, [Online]. Available: Perkin Elmer, https://www.perkinelmer.com. [Accessed Apr 26, 2021].

[20] S. Mestry and S. Mhaske, "Synthesis of epoxy resins using phosphorus-based precursors for flame-retardant coating," *J. Coatings Technology and Research*, vol. 16, no. 3, pp. 807-818, 2019.

[21] W. Qiao, B. Li and Z. Kang, "Differential scanning calorimetry and electrochemical tests for the analysis of delamination of 3PE coatings," *International Journal of Electrochemical Science*, vol. 14, pp 7389-7400, 2019.

[22] J. D. Menczel, L. Judovits, R. B. Prime, H. E. Bair, M. Reading and S. Swier, "Differential Scanning Calorimetry (DSC)," in *Thermal analysis of polymers*, New Jersey: John Wiley & Sons, 2009, pp. 7-240.

[23] W. H. Hsu, "Material Safety Data Sheet ThinFlex-Q (Q2,Q3, Q4, Q5, Q6, Q8, Q9)," Kunshan City: TopFlex Co., 2014, pp. 1-5.

[24] TopFlex Co., "ThinFlex-Q2,Q-0514TA-mb Halogen Free Coverlay," Kunshan City: TopFlex Co., 2014, pp. 1-3.

[25] Determination of Thickness of Metallic Clad Laminates, Cross-sectional 12/94, IPC Standard IPC-TM-650 Test Method Manual 2.2.18.1, 1994.

[26] TGA, IPC Standard IPC-TM-650 Test Method Manual 2.3.40, 1995.

[27] Glass Transition Temperature and Cure Factor by DSC, IPC Standard IPC-TM-650 Test Method Manual 2.4.25, 1994.

[28] D. Kaisarly, M. El Gezawi, P. Rösch and K. -H. Kunzelmann, "Shrinkage vectors and volumetric shrinkage percentage of differently applied

composites," *International Journal of Adhesion and Adhesives*, vol. 105, pp. 102793, 2021.

[29] I. Nevliudov, E. Razumov-Fryzyuk, D. Nikitin, D. Bliznyuk and R. Strelets, "Technology For Creating The Topology Of Printed Circuit Boards Using Polymer 3d Mask," *Innovative Technologies and Scientific Solutions for Industries*, vol. 1, no. 15, pp. 120-131, 2021.

[30] K. Y. Wong, P. J. Liew, K. T. Lau and J. Wang, "Optimization of copper via filling process for flexible printed circuit using response surface methodology," *J. Advanced Manufacturing Technology* (JAMT), vol. 14, no. 2, pp. 1-14, 2020.

[31] G. Wypych, Handbook of polymers, 2nd ed., Toronto: ChemTec Publishing, pp. 117-432, 2016.